Concerted control of *Escherichia coli* cell division

Matteo Osella[a,b,1], Eileen Nugent[c], and Marco Cosentino Lagomarsino[a,b,1]

[a]Centre National de la Recherche Scientifique (CNRS), Unité Mixte de Recherche 7238, F-75006 Paris, France; [b]Genomic Physics Group, Unité Mixte de Recherche 7238 "Computational and Quantitative Biology," Université Pierre et Marie Curie (UPMC) Paris-VI, Sorbonne Universités, F-75006 Paris, France; and [c]Cavendish Laboratory and Nanoscience Centre, University of Cambridge, Cambridge CB3 0HE, United Kingdom

Edited by Nancy E. Kleckner, Harvard University, Cambridge, MA, and approved January 21, 2014 (received for review July 19, 2013)

The coordination of cell growth and division is a long-standing problem in biology. Focusing on *Escherichia coli* in steady growth, we quantify cell division control using a stochastic model, by inferring the division rate as a function of the observable parameters from large empirical datasets of dividing cells. We find that (*i*) cells have mechanisms to control their size, (*ii*) size control is effected by changes in the doubling time, rather than in the single-cell elongation rate, (*iii*) the division rate increases steeply with cell size for small cells, and saturates for larger cells. Importantly, (*iv*) the current size is not the only variable controlling cell division, but the time spent in the cell cycle appears to play a role, and (*v*) common tests of cell size control may fail when such concerted control is in place. Our analysis illustrates the mechanisms of cell division control in *E. coli*. The phenomenological framework presented is sufficiently general to be widely applicable and opens the way for rigorous tests of molecular cell-cycle models.

Cell division control couples growth and division, influencing most aspects of cellular physiology (1). Attempts to address this long-standing question have been limited by restricted experimental access to single-cell attributes (2–5). Even in the simple model organism *E. coli*, a fully quantitative characterization of how cell division time and size are determined is lacking (6), with most attempts dating back to the 1960s (2, 7, 8). Current high-throughput microfluidic techniques enable experiments measuring the attributes of many cells (9) opening up the possibility of testing quantitative models of cell division control.

Cell cycle control is generally described in terms of the two categories of "timer" and "sizer" (5). The precise mechanism in place is determined by examining the scatter plot of the amount of growth within a time interval versus the cell size at the entrance of the interval (we hereafter refer to this plot as "size-growth plot"). *SI Appendix*, Fig. S1, illustrates the dichotomy between a sizer and a timer, and how it can be investigated using a size–growth plot. If a deterministic size threshold ("sizer") exists, a linear fit to the data points (using the logarithm of birth size in case of exponential growth) yields a line with slope −1. If the slope is 0, growth is uncorrelated with the entrance size, indicating that a "timer" description is more appropriate. The rationale for this is the following. The amount of growth in time τ is quantified as $x_f = x_0 e^{\alpha\tau}$ for exponential growth, where x_0 and x_f are the initial and final size, respectively. Assuming that cells must reach a certain size threshold to divide or proceed to the next cell cycle stage would lead to negative correlation between the logarithm of the initial size $\log x_0$ and the product $\alpha\tau$, and more specifically to a slope −1 of the linear fit. By extension of the previous argument, it is thought that intermediate slopes emerging from a size–growth scatter plot correspond to intermediate strengths of size control (5, 10) (also generally called "sizer"). For example, a pioneering study of this kind focused on single yeast cells, using the fluorescence from a reporter gene as a proxy for cell mass (10). This study uncovered the existence of a cell size threshold for entry into a specific cell cycle phase.

Here, we introduce an alternative approach. We consider data of $\sim 10^5$ cell divisions of fast-growing *E. coli* in steady exponential growth (9), and use them to define a fully quantitative phenomenological model of division control. This description goes beyond the timer vs. sizer dichotomy, and can be used to test the dependency of the division rate on all of the measured observables. Specifically, we find that a pure dependency of division rate on cell size does not suffice to reproduce the available experimental observations, but a joint dependency of division rate on size and cell cycle time does.

Results

Main Features of the Experimental Data. The experimental data describe a growth–division process (Fig. 1*A*) where each cell grows exponentially (11) at a rate α (Fig. 1*B*) from an initial size x_0 to a final size x_f during a doubling time τ. Because, in steady-state growth, *E. coli* grows essentially through elongation, we used cell length to quantify growth (2, 9, 12). Fig. 1*B* and *SI Appendix*, Fig. S2, show that the majority of the cells elongate exponentially with time and do not display significant growth rate variations at specific cell cycle stages (13–15) (*SI Appendix*). Hence, a single growth (elongation) rate α, obtained by fitting the plot of length vs. time with an exponential (9) for each cell cycle, is a satisfactory approximation of the single-cell elongation process. In agreement with previous observations (2, 9, 16, 17), histograms of doubling time, growth rate, and size show a substantial degree of cell-to-cell variability even in tightly controlled environmental conditions, with roughly Gaussian growth rate distributions, and right-skewed initial and final size distributions (Fig. 1 *C*–*E*).

Size–Growth Plots Show the Existence of Size Control. Taking the conventional approach to testing for size control, we have considered the size–growth plots of the experimental data. In the case of the *E. coli* data analyzed here, the size–growth plot shows a negative correlation, with slope of the linear fit close to −0.3 (Fig. 2*A*).

Significance

The decisional process controlling cell division is a long-standing question in biology, but the answers were traditionally hindered by limited statistics on single cells. Contemporary experimental tools overcome this problem, but this progress must be combined with new theoretical tools to approach the data. This work introduces a quantitative method for estimating the variables controlling division rate and uses it to construct a minimal model from large-scale dynamic data on the size of dividing *Escherichia coli* cells. Cell size is found to be an important control variable of cell division, but not the sole one. Conversely, a description where division rate is determined jointly by cell size and time into the cell cycle reproduces well the available measurements.

Author contributions: M.O., E.N., and M.C.L. designed research; M.O. and M.C.L. performed research; M.O. contributed new reagents/analytic tools; M.O. analyzed data; and M.O., E.N., and M.C.L. wrote the paper.

The authors declare no conflict of interest.

This article is a PNAS Direct Submission.

[1]To whom correspondence may be addressed. E-mail: mosella@to.infn.it or marco.cosentino-lagomarsino@upmc.fr.

This article contains supporting information online at www.pnas.org/lookup/suppl/doi:10.1073/pnas.1313715111/-/DCSupplemental.

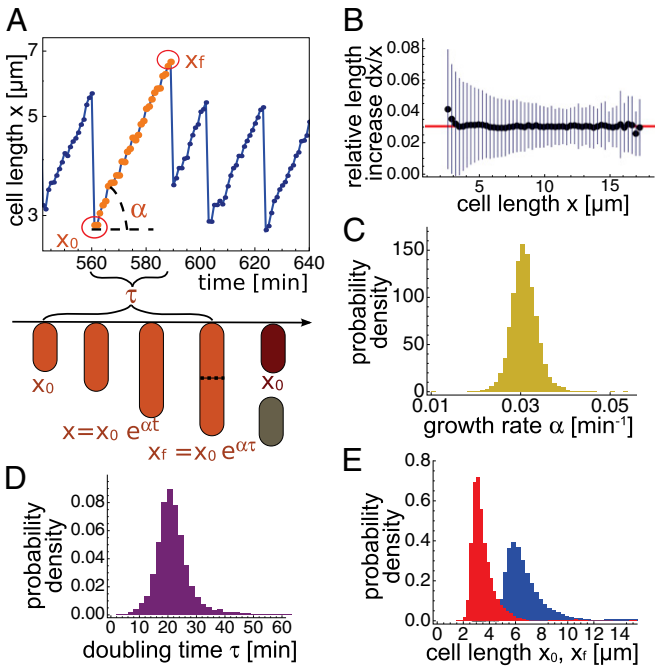

Fig. 1. Empirical constraints on the possible phenomenological models of cell growth and division. (*A*) Illustration of main variables available from data: initial and final length (x_0,x_f), doubling time (τ), and growth rate (α) estimated through an exponential fit of length vs. time. Exponential elongation is observed by the linearity of $\log x$ vs. t (*A*) and by the measured constant relative length increase per unit time (dx/x) as a function of length x (*B*). Here, the length increase is averaged over all cells in the dataset ($\approx 50\times10^3$, strain MG1655 old-pole cells; see *SI Appendix*) and, despite the variability (error bars represent SD), it is compatible with exponential growth, especially between 3 and 10 μm (more than 90% of cells). The continuous red line shows the growth $\langle\alpha\rangle$ obtained through exponential fits of single-cell elongation. (*C*–*E*) Distributions of elongation growth rate α (*C*), doubling time τ (*D*), and cell length (*E*) measured at birth (x_0, red histogram on the left) and at division (x_f, blue histogram on the right).

To investigate in more detail whether this correction of cell size is performed by tuning the elongation rate or the doubling time, we tested the correlation of these two quantities with the (log) initial size (Fig. 2*B*). The results show that the size correction is implemented by adapting the doubling time, rather than the elongation rate. Cells thus tune their doubling time depending on their birth size to achieve an optimal final size. The negative correlation between total elongation and birth size (Fig. 2*A*) is entirely due to a modulation of the doubling time with the elongation rate appearing to be independent of birth size (Fig. 2*B*).

Phenomenological Description of Cell Division Control by Division Rate. To go beyond size–growth scatter plots, we have considered the following mathematical description of the experimental data. The process of growth and division can be formalized as a continuous-time stochastic process where each cell grows with a rate (assumed constant for each cell cycle), and divides with a variable rate, which, in the experiment, is a function of observables such as cell size and age in the cell cycle (*SI Appendix*). Similar formalizations (sometimes named "sloppy sizer" models) have been proposed, with division probability increasing with cell size (7, 17–20). Within this framework, a full description of the process of cell growth and division ultimately reduces to the determination of the instantaneous rate of elongation $h_g = dx/dt$ and the division rate h_d (7). As we have discussed, in the experimental data cell-length growth is approximated very well by an exponential at all cell sizes, but the fitted rate varies from cell to cell. Thus, in the model, we can assume that the elongation rate h_g is linear in the size x. The proportionality factor α can be described as a random variable, because it can vary across cell cycles; experimentally, this variable is represented by the slope of the linear fit of logarithmic size vs. time. The plot in Fig. 1*C* indicates that the distribution of this variable is well approximated by a Gaussian. However, there is no a priori guarantee that this variable should be treated as independent. We have verified that there is no correlation of growth rate with initial size (Fig. 2*B*) and also that the final cell size x_f is not correlated with α (*SI Appendix*, Fig. S3). This information indicates that it is safe to assume in the model that $\alpha = h_g/x$ is an independent random variable extracted from the empirical distribution. We have threfore done so. Hence, the relevant properties of cell division control are all contained in the division rate h_d. The model assumes that at cell division, each cell is divided exactly in half, but we have tested that relaxing this assumption does not affect the main conclusions (see *Necessity of Concerted Control*). The model is illustrated in detail in *SI Appendix*, section S3.

Assuming this description, we can explore whether it can capture the measured data. We start considering the minimal version of this model, where h_d depends only on one parameter, cell size $h_d = h_d(x)$ (7, 17, 18). In this case, we can infer the dependency of the division rate h_d on cell size x directly from empirical data (Fig. 3*A*), by considering the histogram of the fraction of undivided cells reaching a certain size, and inverting the theoretical formula that relates this quantity to the division rate. The full procedure is illustrated in *SI Appendix*, section S3.3. The empirical division rate (Fig. 3*B*) reveals a strong sizer at small sizes ($\lesssim 6$ μm in the dataset analyzed here), with h_d increasing roughly as x^{12}, while the control is gradually released

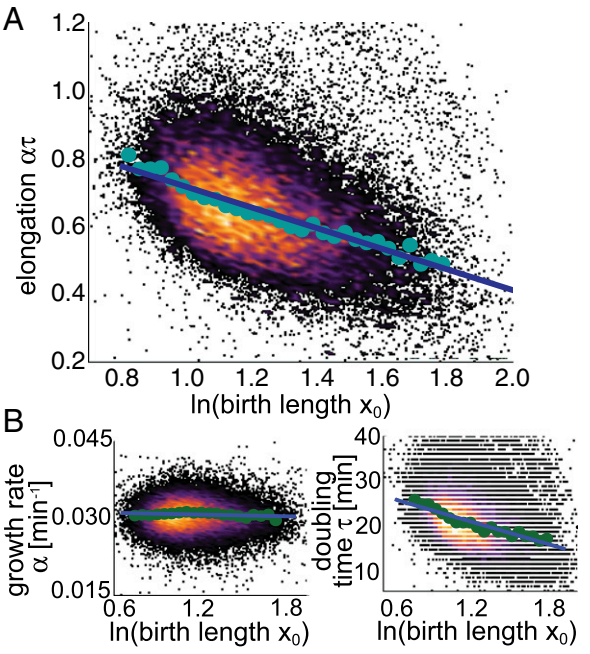

Fig. 2. Size-based division control and size correction by modulating the doubling time. (*A*) The logarithm of birth length x_0 and the cellular elongation $\alpha\tau$ are anticorrelated (Pearson correlation $\simeq -0.38$). The scatter plot is colored by point density, and the large circles are medians on binned data. The slope of the linear fit of medians (continuous blue line) is ~ -0.3, suggesting weak size-based control. (*B*) The correlation between elongation and size at birth is completely accounted for by the anticorrelation between birth size and doubling time (Pearson correlation $\simeq -0.32$) (*Right*). (*Left*) The single-cell growth rate is not correlated with initial size (Pearson correlation $\simeq 0$).

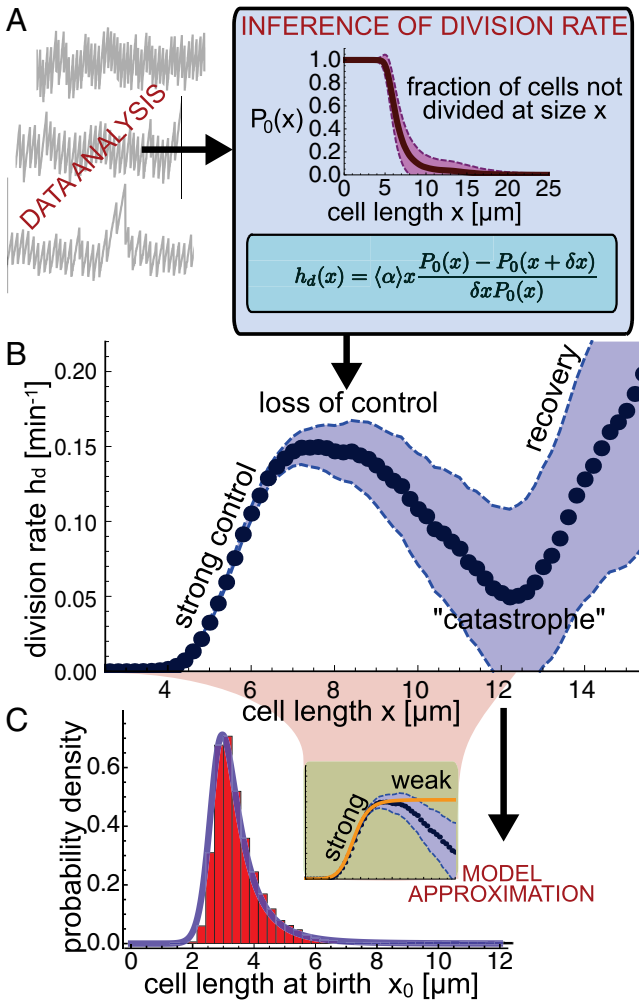

Fig. 3. Inference of the empirical division rate shows a complex size control strategy. (*A*) Schematic of procedure to extract the empirical division rate. We compute the fraction of undivided cells until size x from data ($\approx 50 \times 10^3$ cells in this dataset), estimating the SE as in ref. 21. Shaded area represents the error magnified 100 times. The histogram estimates the "survival probability," and a simple relation connects this quantity with the division rate $h_d(x)$ (*SI Appendix*). (*B*) The estimated division rate as a function of size shows a steep increase at small sizes followed by a saturation. Cells that are still not divided experience a decreasing division rate as their length increases. This escape from the size control is related to the filamentation regime (*SI Appendix*). (*C*) Because the first two regimes account for 90 – 98% of the data (depending on the dataset), a model where the division rate is a Hill function (*Inset*) fits well with the empirical data (red bars) of the distribution of initial cell length. The continuous purple line is an analytical estimate (*SI Appendix*).

for larger cells, as the division rate saturates, until it becomes nearly constant.

There also appears to be a "control catastrophe" region, where the division rate decreases with size. This phenomenon is related to filamentation. A reestablishment of h_d growing with increasing size is visible for cells longer than ~12 μm (the microfluidic channels are $\simeq$ 30 μm long), although the scarcer sampling might cause relevant statistical errors. The phenomenology of division control is consistent across all of the analyzed strains (*SI Appendix*, Fig. S4 *A* and *B*). We find that replicative aging modulates division rate (*SI Appendix*, Fig. S5) in agreement with the previous observation that aging affects the filamentation rate (9) (*SI Appendix*). However, the behavior of aged cells does not differ qualitatively from the rest of the population.

To validate the description of the experimental data assumed above, we solved the quantitative model of cell growth and division numerically and with analytical estimates, and asked whether its predictions could describe the data. In particular, we compared model predictions with three main empirical observables: the distributions of sizes and doubling times, and the correlation between size and elongation (shown by the size–growth plot in Fig. 2*A*). *SI Appendix*, section 3, reports in detail the models analyzed, the analytical calculations, and the procedure of model selection and validation.

A model with the simplifying assumption that the division rate h_d has a power-law dependence on size can reproduce qualitatively empirical size distributions (17). It can also be verified that such a model can yield intermediate slopes in the size–growth plot. However, it is inconsistent with more detailed (previously unavailable) single-cell growth data (*SI Appendix*, Fig. S6). These considerations are relevant to understanding the importance of the transition from strong to weak size control in determining the width and skewness of size distributions. The vast majority of cells are subject to this change in division control regime, with 90% of old-pole cells and 98% of young-pole cells dividing before reaching a length of 9 μm. Therefore, it is natural to test whether a strong size-based division control followed by a relaxation is sufficient to explain both the single-cell growth behavior and the cell size distribution. We found that a model where $h_d(x)$ is a Hill function ($h_d(x) = \frac{k\ x^n}{h^n + x^n}$) fitted on the first part of the empirical plot works rather well (Fig. 3*C*).

Necessity of Concerted Control. However, the model with purely size-based division control is not able to fully capture the empirical distributions of both size and doubling times (Fig. 4), suggesting that further variables, and particularly time in the cell cycle, affect the cell division rate. To shed light on this, we increased the complexity of the model, and assumed that h_d could depend on both size x and time spent in the cell cycle, t, $h_d = h_d(x,t)$. Assuming this model, h_d can be inferred exactly as in the previous one considering the histograms of the fraction of undivided cells of equal size, conditioned on having different values of t, i.e., distinguishing cells of equal size that were born at different times (*SI Appendix*, section S3.3). This analysis (Fig. 4*A*) indicates that cells of equal size modulate their division rate h_d based on the time t spent in the cell cycle, and this result is consistent across different strains (*SI Appendix*, Fig. S4 *C* and *D*). Younger (low t) cells show a decreased division rate compared with older (high t) cells of equal size, in qualitative analogy to what has been found in mammalian cells (4). Therefore, the time elapsed since cell birth appears to play an important role in determining the division rate.

To test whether this theoretical model could reproduce all of the observations, we developed a minimal description for the dependency of h_d on both size and time (Fig. 4*B* and *SI Appendix*, Fig. S7). This model is illustrated in detail in *SI Appendix*, sections S3.1–3. We found that this "concerted control" model captures both the empirical doubling time distribution and the size–growth scatter plot (Fig. 4 *C* and *D*), as well as the cell-size histograms (*SI Appendix*, Fig. S8). As shown by Fig. 4*C* and *SI Appendix*, Fig. S8, the time-based control does not significantly affect the range of cell sizes but plays an important role in the range of possible single-cell doubling times. *SI Appendix*, Fig. S9, recapitulates the comparisons between predictions from the main models considered here and empirical data. Finally, we have verified that relaxing the model assumption of symmetric cell division does not alter the results. *SI Appendix*, Fig. S10, shows that adding stochasticity in the size of daughter cells (as measured from experimental data) does not affect the goodness of the model predictions for size and doubling-time distributions. The asymmetry in size partitioning at division becomes relevant only in the presence of filamentation (9). Because these events

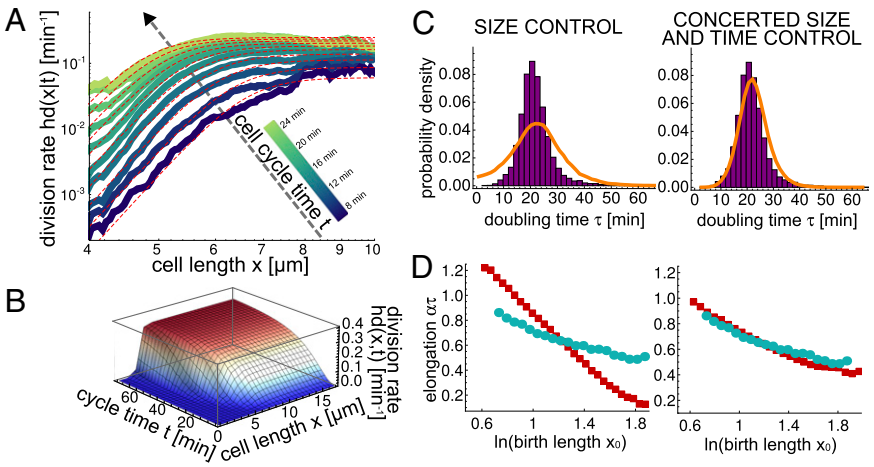

Fig. 4. Evidence of concerted cell division control. (*A*) The empirical division rate at a fixed size depends on the time spent in the cell cycle. The plot is obtained as in Fig. 3 but using histograms conditioned on time *t* within the cell cycle. A Hill function fit of this plot yields parameters that are dependent on *t* (*SI Appendix*). This procedure defines the two-dimensional function $h_d(x,t)$, shown in *B*. The sections of this function (dashed red curves in *A*) reproduce well the estimated division rates at different *t*. (*C*) Comparison of the doubling time distributions from simulations (continuous orange lines) and empirical data (purple histograms). Pure size-based control (Fig. 3) predicts the correct size distribution (Fig. 3*C*) but yields a broader doubling time distribution than the empirical data. Conversely, simulations with the division rate $h_d(x,t)$ shown in *B* reproduce both empirical histograms (*SI Appendix*, Fig. S8). (*D*) The size–growth plot is affected by the presence of time control. Anticorrelation between birth size $log(x_0)$ and elongation $\alpha\tau$ is shown for binned data coming from simulations (red squares) and experiments (blue circles, corresponding to the blue circles in Fig 2*A*). The plots are obtained starting from a scatter plot with the same procedure followed in Fig. 2*A* as the medians of equally sized bins of the *x* axis, starting from experimental data (blue circles) and simulations (red squares). The scatter plots are not shown for graphical clarity. The model with pure size-based control (Fig. 3) predicts a much stronger anticorrelation (*Left*) than the model with concerted control (*Right*).

are rare, our analysis cannot fully capture this phenomenon, and we decided not to include it in the model.

It is important to note that when concerted control is in place, in comparison with pure size control, the traditional test of the presence of a sizer is obscured. Indeed, the size–growth plot shows a decreased correlation (Fig. 4*D*). If one were to use this size–growth plot as a proxy for a "sizer," one would be faced with a paradoxical result: A very strong sizer with strong time modulation of the division probability would show very little correlation in this test, leading to incorrect conclusions. This effect is relevant to the data we analyzed: In the absence of a time–size concerted control, although the model reproduces correctly the size distribution, it predicts a slope of 0.7 in the size-growth plot, i.e., a sizer that is equally strong as that observed for yeast. However, the empirical slope is −0.3, and this is reproduced precisely by the concerted control model (Fig. 4*D*).

Discussion and Conclusions

Although the concepts of timer and sizer are useful, it is now widely accepted that they are insufficient to fully describe size-dependent cell cycle progression, and that new and more precise quantitative tools are needed (5). Here, we have proposed an alternative approach to a classic formalization of this problem as a stochastic process of growth and division, and have shown that it gives a much more stringent quantitative insight into the behavior of the system.

It is interesting to compare our results with what has been shown for yeast, where cell division control has been studied extensively. In the case of *E. coli*, the size–growth plot shows a negative slope of the linear fit close to −0.3 (Fig. 2*A*), which suggests that size control could be weaker than that found in yeast (5, 10, 22). However, the description in terms of division rates sheds more light on the division control. Our analysis indicates that the division control based on size is, in some sense, strong: In fact, as shown in Fig. 4*D*, the slope of the size–growth plot for *E. coli* would be as strong as for yeast if cell division was only conditioned on size. However, we show evidence that, for the *E. coli* data analyzed here, cell division must be conditioned on an extra variable, and that this concerted control affects the slope of the size–growth plot.

Specifically, comparison with model predictions shows that a concerted control based on both time within the cell cycle and size reproduces all of the most important experimental observations (cell size distribution, doubling time distribution, and size–growth plot). Because a similar description is not available for yeast, the question remains open as to whether similar (or different) complex control scenarios, where more than one variable determines the division rate, might be in place.

It is important to stress that the agreement between model prediction and data is not trivially contained in the estimate of the division rate h_d. Indeed, we have shown that a model where the cell division rate inferred from data is assumed to depend on size only, $h_d = h_d(x)$, fails to fully reproduce the experimental observations (the doubling time distribution and the size–growth plot). Also, the fact that the concerted control model with $h_d = h_d(x,t)$ agrees with data does not guarantee that this description is unique. Our preliminary analysis indicates that a model where $h_d = h_d(x,x_0)$ could perform equally well, whereas the inference of $h_d = h_d(x,\alpha)$ through conditioned histograms yields a function that depends only very weakly on α and therefore is nearly equivalent to the case $h_d = h_d(x)$, which does not fully reproduce the empirical observations. Finally, a possible dependency of h_d on three variables, given the constraint of cell growth, is the maximal possible one. For example, a dependency on x, t, α, by the relation $x_0 = x\exp(-\alpha t)$, is equivalent to a dependency on x, x_0, t. To test this dependency, we have considered cumulative histograms of the fraction of undivided cells, doubly conditioned on size and time, with varying α (*SI Appendix*, Fig. S11), and our preliminary results suggest that this effect is weak. However, doubly conditioned histograms are very noisy with the available data. We are addressing these questions in our current work, but systematic data with a wider range of growth rates are likely needed to obtain a full answer.

In addition, we have also shown that the size correction is implemented by adapting the doubling time rather than the elongation rate. A recent work on yeast (23) found a correlation between growth rate in G1 and cell volume at Start (a key event

in the G1/S transition), suggesting a growth-rate-dependent size threshold. This would translate in our case to a correlation between growth rate and final size, which, however, is not present (*SI Appendix*, Fig. S3), marking another difference with yeast.

Our approach defines a quantitative framework with general applicability in the field of cell division control, from bacterial cells all the way up to mammalian and cancer cells. It could also play a role in understanding quantitatively the observed universal features in the cell size distributions of species found in natural ecosystems (20). Importantly, the approach can be extended to infer how the division rate is affected by molecular variables governing the cell cycle, such as expression of key cell cycle regulators or other proxies of cell cycle stage (see *SI Appendix*, section S2, for a detailed discussion). In *E. coli*, these molecular players are well characterized, and obvious candidates are the coupled circuits involving genome replication (and prominently proteins such as DnaA, SeqA, and Hda) (24, 25) and genome segregation and cell division (and proteins such as MinC-D-E, MukB, FtsK, and FtsZ) (26–28). Our full phenomenological characterization of cell division control poses the question of which of these molecules are carrying out the observed regulation and using which regulatory architectures.

Materials and Methods

This section briefly recapitulates the data analysis methods. A detailed description of methods can be found in *SI Appendix*. The publicly available dataset (9) used in this analysis consists of measurements of cell size from segmented images of cells taken at 1-min time intervals. The cells grow in steady exponential conditions in a microfluidic device made of micrometer-sized channels. The dataset collects measurements relative to four different strains: SJ108 and SJ119 (*E. coli* B/r), *E. coli* MG1655 (CGSC 6300), and MG1655 lexA3. Data from different strains were analyzed separately. Cell lineages were separated depending on the age of the cell poles to analyze the effect of replicative aging on division control (*SI Appendix*, Fig. S5). The figures presented in the main text refer to the analysis of old-pole cells (cells at the bottom of every microchannel) of *E. coli* MG1655. The model used for the analysis was accessed by both theoretical estimates and direct simulation. It is defined by two main ingredients: an instantaneous elongation rate h_g and a division rate h_d. See *SI Appendix* for a discussion of the model calculations and the details of the theoretical procedure used to define the functional forms of the rates.

ACKNOWLEDGMENTS. We are very grateful to A. Celani, P.A. Wiggins, and J. Grilli for helpful discussions, to S. Jun for discussions and help with the Wang et al. data, and to Y. Wakamoto, B. Sclavi, G. Fischer, J. Herrick, K.D. Dorfman, N. Kleckner, and S. A. Teichmann for feedback on this manuscript. This work was supported by the International Human Frontier Science Program Organization Grant RGY0069/2009-C.

1. Leslie M (2011) Mysteries of the cell. How does a cell know its size? *Science* 334(6059): 1047–1048.
2. Schaechter M, Williamson JP, Hood JR, Jr., Koch AL (1962) Growth, cell and nuclear divisions in some bacteria. *J Gen Microbiol* 29(3):421–434.
3. Kirschner MW, et al. (2011) Fifty years after Jacob and Monod: What are the unanswered questions in molecular biology? *Mol Cell* 42(4):403–404.
4. Tzur A, Kafri R, LeBleu VS, Lahav G, Kirschner MW (2009) Cell growth and size homeostasis in proliferating animal cells. *Science* 325(5937):167–171.
5. Turner JJ, Ewald JC, Skotheim JM (2012) Cell size control in yeast. *Curr Biol* 22(9): R350–R359.
6. Chien AC, Hill NS, Levin PA (2012) Cell size control in bacteria. *Curr Biol* 22(9): R340–R349.
7. Anderson EC, Bell GI, Petersen DF, Tobey RA (1969) Cell growth and division. IV. Determination of volume growth rate and division probability. *Biophys J* 9(2): 246–263.
8. Painter PR, Marr AG (1968) Mathematics of microbial populations. *Annu Rev Microbiol* 22:519–548.
9. Wang P, et al. (2010) Robust growth of *Escherichia coli*. *Curr Biol* 20(12):1099–1103.
10. Di Talia S, Skotheim JM, Bean JM, Siggia ED, Cross FR (2007) The effects of molecular noise and size control on variability in the budding yeast cell cycle. *Nature* 448(7156):947–951.
11. Godin M, et al. (2010) Using buoyant mass to measure the growth of single cells. *Nat Methods* 7(5):387–390.
12. Margolin W (2009) Sculpting the bacterial cell. *Curr Biol* 19(17):R812–R822.
13. Goranov AI, et al. (2009) The rate of cell growth is governed by cell cycle stage. *Genes Dev* 23(12):1408–1422.
14. Kafri R, et al. (2013) Dynamics extracted from fixed cells reveal feedback linking cell growth to cell cycle. *Nature* 494(7438):480–483.
15. Son S, et al. (2012) Direct observation of mammalian cell growth and size regulation. *Nat Methods* 9(9):910–912.
16. Wakamoto Y, Ramsden J, Yasuda K (2005) Single-cell growth and division dynamics showing epigenetic correlations. *Analyst (Lond)* 130(3):311–317.
17. Hosoda K, Matsuura T, Suzuki H, Yomo T (2011) Origin of lognormal-like distributions with a common width in a growth and division process. *Phys Rev E Stat Nonlin Soft Matter Phys* 83(3 Pt 1):031118.
18. Tyson JJ, Diekmann O (1986) Sloppy size control of the cell division cycle. *J Theor Biol* 118(4):405–426.
19. Rading M, Engel T, Lipowsky R, Valleriani A (2011) Stationary size distributions of growing cells with binary and multiple cell division. *J Stat Phys* 145(1):1–22.
20. Giometto A, Altermatt F, Carrara F, Maritan A, Rinaldo A (2013) Scaling body size fluctuations. *Proc Natl Acad Sci USA* 110(12):4646–4650.
21. Wheals AE (1982) Size control models of *Saccharomyces cerevisiae* cell proliferation. *Mol Cell Biol* 2(4):361–368.
22. Sveiczer A, Novak B, Mitchison JM (1996) The size control of fission yeast revisited. *J Cell Sci* 109(Pt 12):2947–2957.
23. Ferrezuelo F, et al. (2012) The critical size is set at a single-cell level by growth rate to attain homeostasis and adaptation. *Nat Commun* 3:1012.
24. Donachie WD, Blakely GW (2003) Coupling the initiation of chromosome replication to cell size in *Escherichia coli*. *Curr Opin Microbiol* 6(2):146–150.
25. Grant MAA, et al. (2011) DnaA and the timing of chromosome replication in *Escherichia coli* as a function of growth rate. *BMC Syst Biol* 5:201.
26. Reyes-Lamothe R, Nicolas E, Sherratt DJ (2012) Chromosome replication and segregation in bacteria. *Annu Rev Genet* 46:121–143.
27. Bates D, Kleckner N (2005) Chromosome and replisome dynamics in *E. coli*: Loss of sister cohesion triggers global chromosome movement and mediates chromosome segregation. *Cell* 121(6):899–911.
28. Egan AJF, Vollmer W (2013) The physiology of bacterial cell division. *Ann N Y Acad Sci* 1277:8–28.